INCLUSION OF PREEQUILIBRIUM CALCULATION INTO HIGH ENERGY TRANSPORT CODE

K.ISHIBASHI, H.TAKADA,* Y.YOSHIZAWA,** N.MATSUFUJI, T.NAKAMOTO, Y.WAKUTA and Y.NAKAHARA*
Department of Nuclear Engineering, Kyushu University
Hakozaki, Fukuoka 812, Japan
*Japan Atomic Energy Research Institute
Tokai-mura, Ibaraki 319-11, Japan
**Mitsubishi Research Institute, Inc.
Ote-machi, Chiyoda-ku, Tokyo, 100 Japan

ABSTRACT

The High Energy Transport Code (HETC) has been widely used for engineering purposes. We incorporate the preequilibrium calculation into the HETC with a smooth connection to the cascade process. The preequilibrium process is introduced to retain a clear physical meaning both in the connection method and in the initial number of particles and holes. The calculation results are compared with the experimental preequilibrium spectra which have been decomposed from experimental data by the moving source model. Computation results successfully reproduce the backward neutron spectra particularly for incident proton energies below about 100MeV.

I. INTRODUCTION

A great number of energetic neutrons are produced through the spallation reaction when a target is bombarded by high energy protons of about 1 GeV. The reaction is useful for facilities providing the intense spallation neutron sources or transmuting long-lived radioactive wastes[1]. Some computer codes have been developed for designing these spallation facilities. Nucleon Meson Transport Code (NMTC)[2,3] and High Energy Transport Code (HETC)[4-6] are famous as Monte-Carlo particle-transport codes in analyzing the neutron behavior in thick target systems. The codes consist of two types of calculations, i.e. nuclear reaction and interatomic particle transport. The present paper deals only with the nuclear reaction calculation and accordingly concerns itself with the experimental data taken by the use of thin targets.

For performing the calculation of nuclear reactions, the above transport codes make use of the same program MECC-7, which was originally developed by Bertini[7]. The code MECC-7 utilizes a Monte-Carlo algorithm, and the nuclear calculation is based on the intranuclear-cascade evaporation model, where the computation is divided into two steps of intranuclear-cascade and evaporation processes. This model is called a two-step model in the present study. The program to be used in this study is HETC-KFA2(contained in HERMES[8]) which is the modified version of MECC-7. The major modification was incorporation of the high-energy fission, and the detailed table for level-density parameter.

The two-step model has usually been applied to the reaction for the incident proton energies of 20 to 3000 MeV. This model reproduces the overall characteristics of the nuclear reaction fairly well[9]. Nevertheless, the discrepancy in neutron spectra appears at incident proton energies below or about 113 MeV[10], particularly in the backward direction. The existence of the preequilibrium effects in the neutron spectra has been pointed out by Tsukada and Nakahara[11]. The inclusion of the preequilibrium process is considered to be useful in reproducing the neutron spectra. Nakahara and Nishida[12] were interested in the introduction of the preequilibrium process for describing the spallation reaction, and described the Monte Carlo algorithm for the exciton model calculation. The preequilibrium calculation coupled with HETC was preliminarily attempted at Kyushu University- JAERI[13], and also preformed by Prael at LANL[14].

Experimental spallation neutron data have recently been systematically analyzed[15] by a moving source model, and decomposed into three spectra of the cascade, preequilibrium and evaporation processes. In this paper, we compare the preequilibrium calculation results with the decomposed preequilibrium spectra, and adjust preequilibrium parameters to reproduce the preequilibrium spectra. The present code includes the preequilibrium process into the conventional cascade-evaporation calculation, and constitutes a three-step precedure as follows:

First, the cascade calculation is performed with the standard routines, and is terminated by the use of a simple probability function. Subsequently, the exciton-model calculation is executed by taking into account the exact number of excitons as generated in the preceding cascade process. The evaporation process is then conducted as a last step. The present three-step model is applied to the reaction of incident proton energies down to 25 MeV in this study.

II. THREE STEP MODEL

1. Cascade calculation

The cascade calculation in the present study is made on the basis of the Monte-Carlo program code HETC-KFA2, where the intranuclear-cascade model is the same as that of the code originally developed by Bertini[7]. The model assumes that the high-energy incident particle is scattered by intranuclear nucleons in a binary collision. Additional collisions are induced in series by the scattered or recoiled particles, resulting in formation of a collision cascade in the nucleus. The cross section measured for free particles is assumed to be applicable to each collision during the cascade development. The momentum of the intranuclear nucleons is sampled according to the degenerated Fermi distribution with zero temperature. The Monte-Carlo calculation of each cascade history is terminated on conditions where particles are emitted from the nucleus or their kinetic energy falls below a specified value. This value is defined as the sum of a cut-off energy E_c and the nuclear potential depth at the particle location. In the standard setting, E_c is 0 MeV for neutrons, whereas for protons it is the classical Coulomb barrier height.

The original termination of the cascade calculation is modified in the present study. The experimental neutron emission data were decomposed[11,15] into the processes of cascade, preequilibrium and evaporation components. For emission of neutrons possessing energies below about 30 MeV, neutrons originating from the cascade process contribute to the cross section to a very small extent[11]. To take this result into account, a probability density function $f(E_c)$ is introduced into the cascade calculation to suppress the emission cross section of the low-energy cascade neutrons. This function determines the cut-off energy E_c at terminating the calculation of each cascade history. The function is written by

$$f(E_c) = 2\, E_0^{-1}\, (1-E_c/E_0) \ , \qquad (1)$$

where E_0 is an adjustable parameter. The value of E_c is then randomly chosen from 0 to E_0 according to Eq. (1). When the particle moving in the nucleus has a kinetic energy below the specified value dependent on the chosen quantity of E_c, the calculation for the particle is terminated. For protons, the cut-off energy E_c is sampled in the same way, but if the sampled value is below the Coulomb barrier height, it is substituted by the barrier energy.

The nuclear phenomenon arising near the end of the cascade process has not so far been elucidated in the proton-induced spallation reaction. As an approach to studying a physical indication of Eq. (1), a particle emission probability is calculated by assuming the applicability of the exciton model[16] to this phenomenon. The description is given in ref. 13. When the two-particle one-hole state is presumed together with the Kalbach constant of K= 500MeV^3, the results of the neutron emission probability are consistent with those deduced by Eq. (1) with E_0=40 MeV. The value of E_0=40 MeV is used in the following calculation. The termination method based on Eq. (1) is supposed to be some correction of the cascade model with regard to the kind of preequilibrium effect.

2. Preequilibrium calculation by a Monte Carlo algorithm

After the above cascade process, the calculation of the preequilibrium process is carried out as the second step. The exciton model is adopted in this process because of its simplicity in computation. The principle of the calculation is basically the same as that described by Gudima et al.[17] In the present study, the master equation is solved by a Monte Carlo algorithm[12]. The flow chart is shown in Fig. 1, where the symbols appearing there are summarized in Table 1. At the beginning of this process, such values of the nucleus as mass number A, atomic number Z, and excitation energy E are brought from the cascade calculation. For nuclear quantum state, neither the angular momentum nor the spin is considered in the preequilibrium and the further evaporation process.

Gudima et al. have assumed the state of two particles and one hole at the start of the preequilibrium process. At high incident energies, however, many particles and holes are already present after the cascade process. The number of these excitons often exceeds ten at an incident proton energy above a few hundred MeV. At the beginning of the preequilibrium calculation, we adopt the exact numbers of particles (p) and holes (h) as generated in the preceding cascade calculation. Computation is made to obtain probabilities for exciton-number increase λ_+, unchange λ_0, decrease λ_-, and particle emission Γj. The event to be encountered is chosen by a random sampling, and subsequently processed by a suited subroutine. For particle emission, both the kinetic energy T and the emission angle θ are random-sampled according to their probability density function. The Gudima formalism contains no adjustable parameter for evaluating the transition rates of λ_+, λ_0 and λ_-. We then multiplied the rates by an adjustable factor F of 2.5. The preequilibrium calculation is terminated when the number of excitons n=p+h exceeds the minimum of a termination value of 15 to 25 and the equilibrium value of $n_{eq}=(2gE)^{1/2}$.

For the angular distribution of neutron emission, Gudima et al. solved the master equation with consideration of the angular dependence. In this study, for simplicity of the calculation, the angular distribution of neutrons is obtained by an empirical method. Kalbach[18] showed the systematics for the angular distribution. We utilized the same function, i.e. combination of hyperbolic- sine and cosine, to reproduce the preequilibrium angular distribution. In our case, however, the angular distribution is almost isotropic and the value a of Kalbach was changed to 0.035a+0.05.

3. Evaporation calculation

After the preequilibrium process, the nuclei are left in a high excitation state. Either nucleons or light nuclei are emitted in the evaporation process as the third step. For choosing the type and energy of the emitted particles, the Weisskopf formula is used in computation. The formula requires the level density parameter for the calculation of the emission probabilities. The detailed compilation values of the level-density parameter[6,19] were used as the automatic choice of HETC-KFA2.

III. CALCULATION RESULTS

Typical calculational results by the present model are compared with those by the conventional two-step model in Fig. 2. The parameters in the calculation are summarized in Table 2. In this figure, the neutron spectra at 60 deg are plotted for incident protons of 113 MeV on lead. The spectra are shown for each process. Emission of the cascade neutrons with energies below 30 MeV is considerably suppressed in the three-step model in contrast to the case of the two-step one. As seen in the results of the three-step model, the preequilibrium process yields neutrons of energies dominantly up to 20 MeV, while the evaporation one produces those of a few to several MeV. The experimental neutron data for thin targets by 113 MeV protons[10] were decomposed into three components by the moving source model[15]. The decomposition is considered to be useful for detailed study of the preequilibrium process. The results for lead are shown in Figs. 3 to 5, and those for iron in Figs. 6 to 8. Marks indicate the decomposed experimental data, and lines stand for calculation results. The decomposed data are reproduced by the three-step calculation, with the exception of some underestimation of the evaporation component.

The experimental neutron spectra[10] are shown by marks in Fig. 9 for lead. The dashed lines represent the calculational results of the two-step model. The differences between the dashed lines and the experimental data are as follows: In the backward direction of 150 deg, the dashed line is appreciably lower than the experimental result in the region above 10 MeV. The experimental spectra at 30 and 60 deg at energies around 10 MeV are overestimated by the two-step calculation.

The computation results by the three-step model are shown by the solid lines in Fig. 9. In the direction of 150 deg, the solid line agrees with the experimental spectrum for the neutrons with energies especially above 10 MeV. This agreement originates from inclusion of the preequilibrium process. The solid lines coincide with the dashed ones at around 10 MeV at angles of 30 and 60 deg: The reduction of cascade neutron emission in this region is reasonably

compensated by the preequilibrium calculation, as deduced by Fig. 2. At a few to several MeV, the solid lines are slightly lower than the dashed ones. In spite of some disagreement of the cross section in the evaporation process, as a whole, it can be said that the solid lines reproduce the experimental data well, especially in the backward direction. The results for iron are shown in Fig. 10. The three-step calculation reproduces the experimental data mostly better than the two-step one.

The results for 25.5 MeV proton incident on lead[20] are shown in Fig. 11. The dashed lines by the two-step calculation appreciably underestimate the experimental cross section in the backward direction. The cascade calculation at such low incident energy tends to produce the forward-peak angular distribution that is not seen in the experimental data. Since the pre-equilibrium process shows more isotropic angular distribution than the cascade process, the backward neutron cross section is greatly improved by adoption of the preequilibrium calculation. For 256[21] and 800 MeV[9] proton incidence on lead, the results are shown in Figs. 12 and 13, respectively. The solid lines by the three-step model in Fig. 13 almost coincide with the dashed ones: The results of the present three-step calculation approaches those of the cascade evaporation model with increasing incident energy.

IV. CONCLUSION

The spallation reaction was calculated by the three-step model composed of the cascade, preequilibrium and evaporation processes. The cascade calculation was performed by counting the number of particles and holes, and was terminated by means of the simple probability function. In the second step of the preequilibrium process, the exciton-model calculation was made with the Monte-Carlo algorithm. The initial number of excitons was brought from the preceding cascade calculation. Parameters for the preequilibrium process were adjusted with reference to the preequilibrium spectra which had been derived from decomposing the experimental 113 MeV proton-incident data. The three-step calculation was made for the reaction induced by protons of 25 to 800 MeV on iron and lead. This model was particularly useful for reproducing the backward neutron spectra at incident proton energies around or below 100 MeV. At higher proton energies, the results of the present model approach those of the standard cascade-evaporation model.

ACKNOWLEDGMENTS

The authors gratefully acknowledge Dr. D. Filges of KFA and F. Atchison of PSI for supplying their versions of the HETC.

REFERENCES

(1) T.Nishida et al.: JAERI-M 90-025 (1990) 343.
(2) W.A.Coleman and T.W.ARMSTRONG: Nucl.Sci.Eng. 43 (1971) 353.
(3) Y.Nakahara and T.Tsutsui: JAERI-M 82-198 (1982).
(4) T.W.Armstrong et al.: Nucl.Sci Eng. 49 (1972) 82.
(5) F.Atchison: RL-81-006 (1981).
(6) D.Filges et al.: Phys. Rev. C36 (1987) 1988.
(7) H.W.Bertini: Phys. Rev. C6 (1973) 631.
(8) P.Cloth et al.: "HERMES (High Energy Radiation Monte Carlo Elaborate System, " KFA-IRE-E AN/12/88 1988".
(9) W.Amian et al.: Nucl.Sci.Eng. 112 (1992) 78.
(10) M.M.Meier et al.: Nucl. Sci. Eng. 102 (1989) 310.
(11) K.Tsukada, Y.Nakahara: Atomkernenerg. • Kerntech. 44 (1984) 186.
(12) Y.Nakahara, T.Nishida: JAERI-M 86-074 (1986).
(13) N.Ishibashi et al.: JAERI-M 90-025 (1990) 362.
(14) R.E.Prael: "Model Cross Section Calculations Using LAHET", presented at Symposium on Nuclear Data Evaluation Methodology, October 1992, BNL.
(15) K.Ishibashi et al.: J.Nucl.Sci.Technol. 29 (1992) 499.
(16) C.C.Kalbach: Nucl. Phys. A210 (1973) 590.
(17) K.K Gudima et al: Nucl.Phys. A401, (1983) 329.
(18) C.Kalbach: Phys. Rev. C37 (1988) 2350.
(19) H.Baba et al: Nucl.Phys. A159, (1970) 625.

(20) K.Harder et al.: Hamburg University HH87-01 (1987)
(21) M.M.Meier et al.: Nucl.Sci.Eng. 104 (1990) 339.

Table 1 Nomenclature of the symbols in Fig. 1 for the exciton model calculation.

A	:	Mass number
Z	:	Atomic number
E	:	Excitation energy (MeV)
p	:	Number of particles
h	:	Number of holes
n	:	Total number of excitons
n_{eq}	:	Equilibrium number of excitons
g	:	Single particle level density (MeV^{-1})
λ_+	:	Interaction rate of increase in the number of excitons (s^{-1})
λ_0	:	Interaction rate of unchange in the number of excitons (s^{-1})
λ_-	:	Interaction rate of decrease in the number of excitons (s^{-1})
Γj	:	Emission rate of particle j integrated over energy (s^{-1})
$\Gamma j(T)$	:	Emission rate of particle j per kinetic energy ($s^{-1}MeV^{-1}$)
r	:	Random number
T	:	Kinetic energy of particle (MeV)
B_j	:	Binding energy of particle (MeV)
θ	:	Emission angle of particle (deg)
$\Theta n(T,\theta)$	:	Probability density function for neutron-emission angular-distribution (deg^{-1})

Table 2 Summary of the major parameters used in the two- and three-step models.

Process	Two-step model	Three-step model
Cascade		
Cut-off energy (E_c)	Neutron: 0 MeV Proton: Half of potential barrier	Eq.(1) Sampling by Eq.(1) with constraint of the left energy as the lowest.
Preequilibrium		
Emission probability	None	According to Gudima et al.[17] with correction of $\lambda_+ / \lambda_0 / \lambda_-$
Angular distribution	None	According to Kalbach[18] with correction of a
Evaporation		
Level density	Compiled results in HETC/KFA [6]	

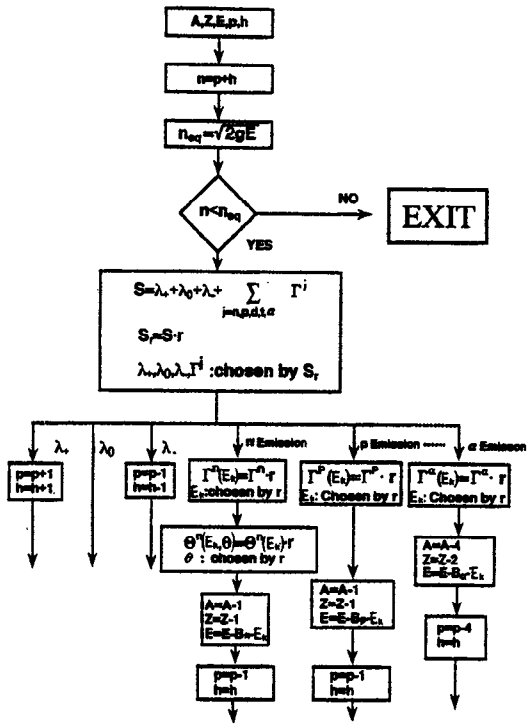

Fig.1 Flow chart for solving the master equation of the exciton model. The symbols are explained in Table 1.

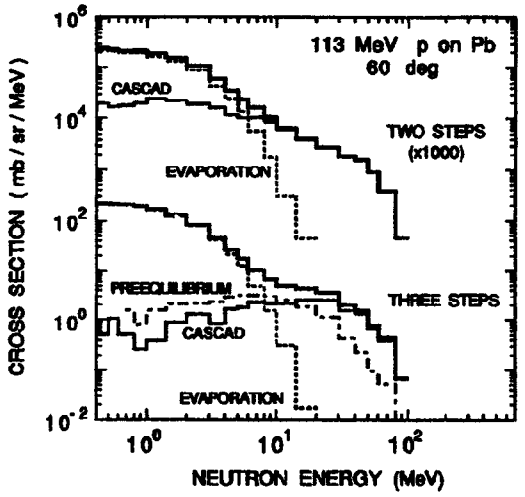

Fig.2 Decomposed neutron spectra obtained in the two- and three-step calculations.

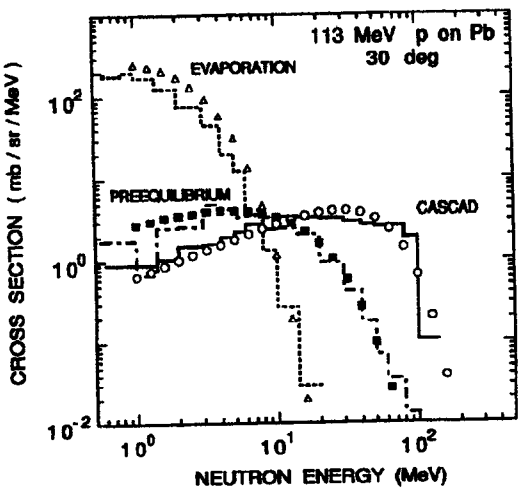

Fig.3 Decomposed neutron spectra for the 113MeV proton incidence on lead at 30deg. The marks stand for the experimental spectra analyzed by the moving source model.

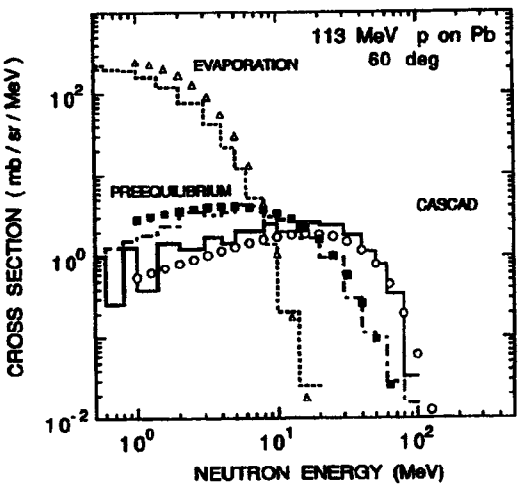

Fig.4 Decomposed neutron spectra for lead at 60deg.

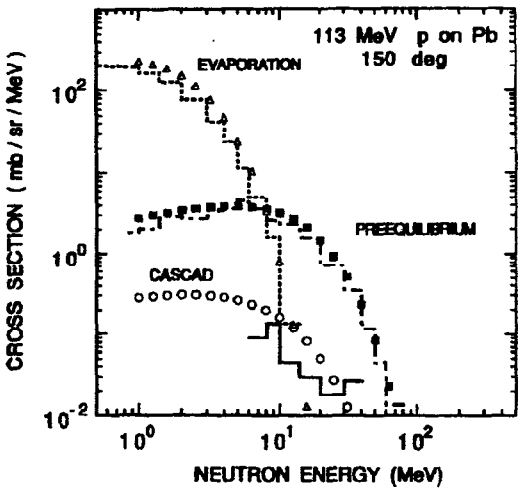

Fig.5 Decomposed neutron spectra for lead at 150deg.

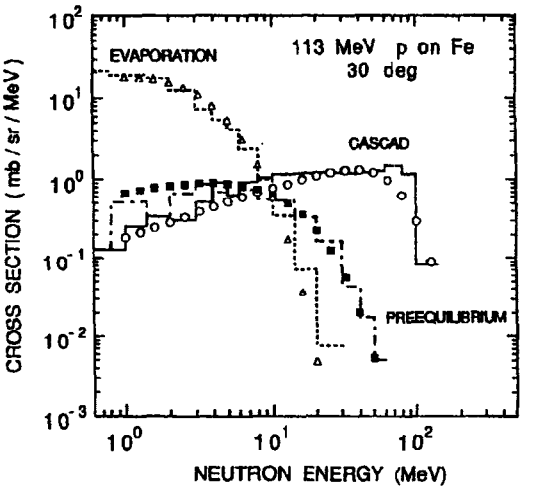

Fig.6 Decomposed neutron spectra for iron at 30deg.

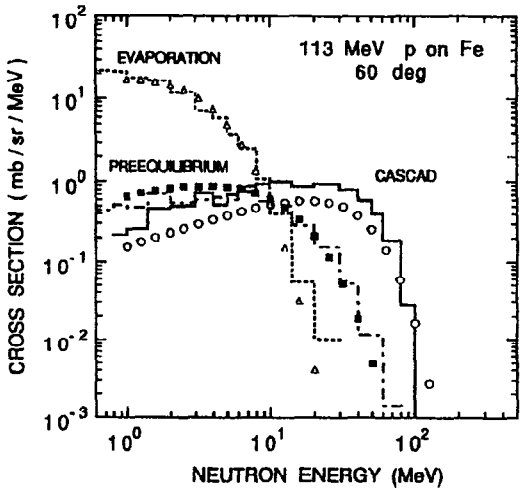

Fig.7 Decomposed neutron spectra for iron at 60deg.

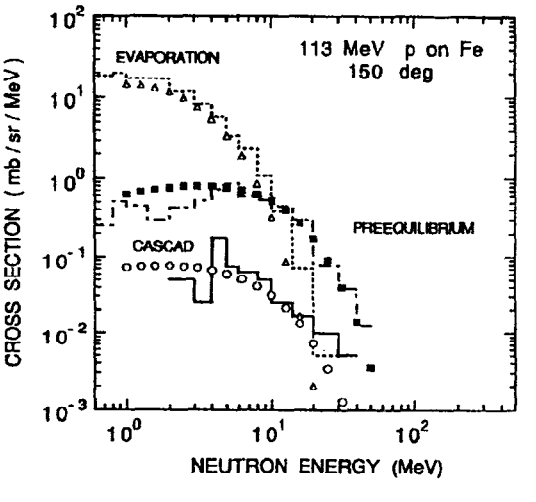

Fig.8 Decomposed neutron spectra for iron at 150deg.

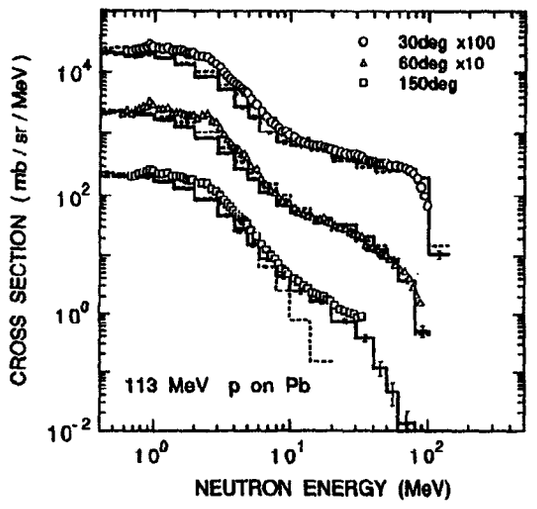

Fig.9 Double differential cross section for the 113MeV proton incidence on lead. Cross marks indicate the experimental data[10]. Dashed and solid lines show the two- and three-step calculations, respectively.

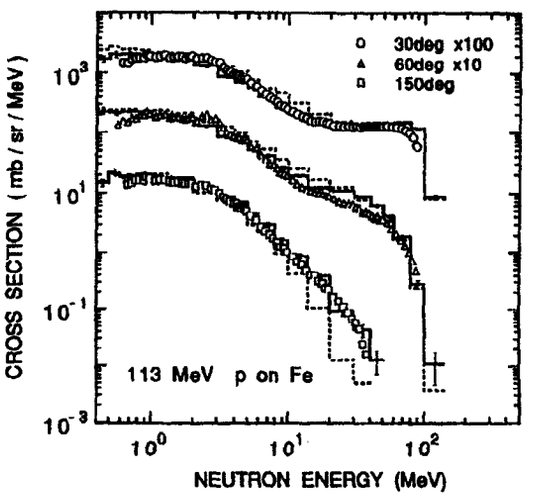

Fig.10 Experimental[10] and calculational double differential cross section for the 113MeV proton incidence on iron.

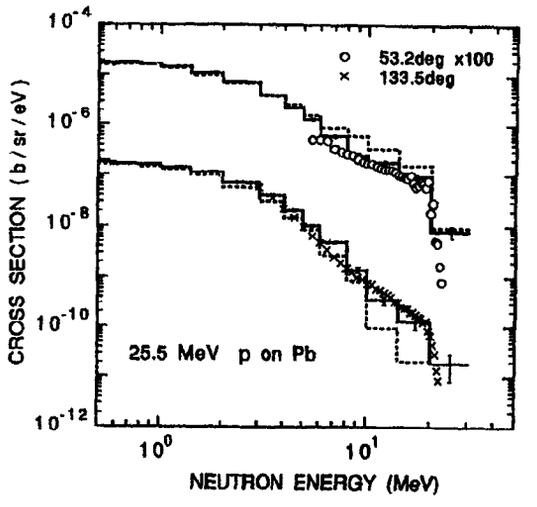

Fig.11 Experimental[20] and calculational double differential cross section for the 25.5MeV proton incidence on lead.

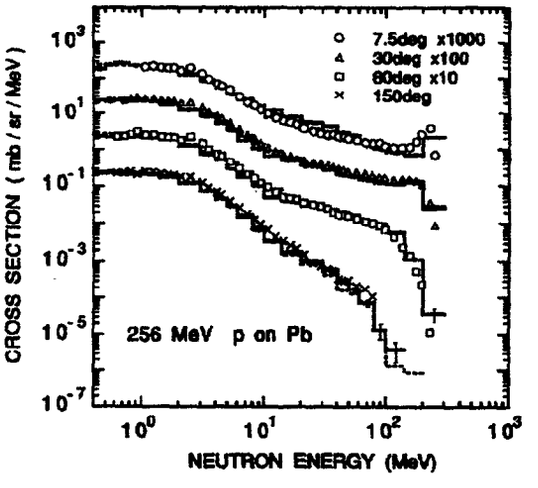

Fig.12 Experimental[21] and calculational double differential cross section for the 256MeV proton incidence on lead.

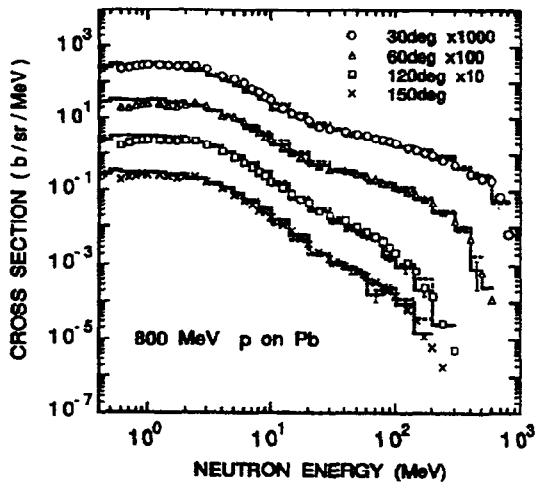

Fig.13 Experimental[9] and calculational double differential cross section for the 800MeV proton incidence on lead.